

Effect of direct reaction channels on deep sub-barrier fusion in asymmetric systems

Md. Moin Shaikh,¹ S. Nath,^{1,*} J. Gehlot,¹ Tathagata Banerjee,¹ Ish Mukul,^{1,†} R. Dubey,^{1,‡} A. Shamlath,² P. V. Laveen,² M. Shareef,² A. Jhingan,¹ N. Madhavan,¹ Tapan Rajbongshi,^{3,§} P. Jisha,⁴ G. Naga Jyothi,⁵ A. Tejaswi,⁵ Rudra N. Sahoo,⁶ and Anjali Rani⁷

¹*Nuclear Physics Group, Inter University Accelerator Centre,
Aruna Asaf Ali Marg, Post Box 10502, New Delhi 110067, India*
²*Department of Physics, School of Mathematical and Physical Sciences,
Central University of Kerala, Kasaragod 671314, India*

³*Department of Physics, Gauhati University, Guwahati 781014, India*

⁴*Department of Physics, University of Calicut, Calicut 673635, India*

⁵*Department of Nuclear Physics, Andhra University, Visakhapatnam 530003, India*

⁶*Department of Physics, Indian Institute of Technology Ropar, Rupnagar 140001, Punjab, India*

⁷*Department of Physics and Astrophysics, University of Delhi, Delhi 110007, India*

(Dated: July 17, 2022)

A steeper fall of fusion excitation function, compared to the predictions of coupled-channels models, at energies below the lowest barrier between the reaction partners, is termed as deep sub-barrier fusion hindrance. This phenomenon has been observed in many symmetric and nearly-symmetric systems. Different physical origins of the hindrance have been proposed. This work aims to study the probable effects of direct reactions on deep sub-barrier fusion cross sections. Fusion (evaporation residue) cross sections have been measured for the system $^{19}\text{F}+^{181}\text{Ta}$, from above the barrier down to the energies where fusion hindrance is expected to come into play. Coupled-channels calculation with standard Woods-Saxon potential gives a fair description of the fusion excitation function down to energies $\simeq 14\%$ below the barrier for the present system. This is in contrast with the observation of increasing fusion hindrance in asymmetric reactions induced by increasingly heavier projectiles, *viz.* ^6Li , ^{11}B , ^{12}C and ^{16}O . The asymmetric reactions, which have not shown any signature of fusion hindrance within the measured energy range, are found to be induced by projectiles with lower α break-up threshold, compared to the reactions which have shown signatures of fusion hindrance. In addition, most of the Q -values for light particles pick-up channels are negative for the reactions which have exhibited strong signatures of fusion hindrance, *viz.* $^{12}\text{C}+^{198}\text{Pt}$ and $^{16}\text{O}+^{204,208}\text{Pb}$. Thus, break-up of projectile and particle transfer channels with positive Q -values seem to compensate for the hindrance in fusion deep below the barrier. Inclusion of break-up and transfer channels within the framework of coupled-channels calculation would be of interest.

PACS numbers: 24.10.Eq, 24.50.+g, 25.70.Jj

Fusion between two nuclei at near barrier energies have been studied quite extensively in last few decades [1–4]. Fusion cross sections (σ_{fus}) have been found to be enhanced at sub-barrier energies in comparison with the predictions of one-dimensional barrier penetration model (1D-BPM). Coupling between the relative motion in the entrance channel, the intrinsic degrees of freedom of the participating nuclei and nucleon transfer channels has been invoked to explain the measured fusion excitation functions. Extending the measurements towards lower energies has immense astrophysical significance as accurate knowledge of the reaction rates at very low energies might aid in answering some of the open questions in big bang nucleosynthesis.

Jiang *et al.* [5] had first observed a steeper fall of σ_{fus} at deep sub-barrier energies in the reaction $^{60}\text{Ni}+^{89}\text{Y}$, which could not be explained by the coupled-channels (CC) calculation with standard potential parameters. Subsequently, similar observations have been reported for many other symmetric and nearly-symmetric light [6, 7], medium-light [8–17] and medium-heavy [18–22] systems with some exceptions [9, 14, 16, 22–25]. Two different representations of measured σ_{fus} have been proposed to conclude about fusion hindrance without recourse to model predictions: (a) the logarithmic derivative of the energy-weighted cross section [5], *viz.*,

$$L(E_{\text{c.m.}}) = \frac{d[\ln(E_{\text{c.m.}}\sigma)]}{dE_{\text{c.m.}}} = \frac{1}{E_{\text{c.m.}}\sigma} \frac{d(E_{\text{c.m.}}\sigma)}{dE_{\text{c.m.}}} \quad (1)$$

and (b) the astrophysical S -factor [18], *viz.*,

$$S(E_{\text{c.m.}}) = E_{\text{c.m.}}\sigma(E_{\text{c.m.}})\exp(2\pi\eta). \quad (2)$$

Here $E_{\text{c.m.}}$ and η are the energy available in the centre of mass (c.m.) frame of reference and the Sommerfeld parameter, respectively. Observation of continuous increase of $L(E_{\text{c.m.}})$ with decreasing $E_{\text{c.m.}}$ and a maximum

* subir@iuac.res.in

† Presently at TRIUMF, 4004 Wesbrook Mall, Vancouver, British Columbia, V6T 2A3, Canada

‡ Presently at iThemba LABS, National Research Foundation, PO Box 722, 7129 Somerset West, South Africa

§ Presently at Department of Physics, Handique Girls' College, Guwahati 781001, Assam, India

of $S(E_{c.m.})$ is considered the clearest signatures of deep sub-barrier fusion hindrance.

A threshold energy has been worked out from systematics [26], below which fusion hindrance is expected to be observed:

$$E_s(\zeta) = 0.356 \zeta^{\frac{2}{3}} \text{ MeV}; \quad (3)$$

$$L_s(\zeta) = 2.33 \text{ MeV}^{-1}, \quad (4)$$

where $\zeta = Z_p Z_t \sqrt{\frac{A_p A_t}{A_p + A_t}}$ is a parameter characterizing the size of the colliding system; Z_p (Z_t) and A_p (A_t) being the atomic and the mass number of the projectile (target), respectively.

A host of different theoretical approaches has been attempted to explain the observed change of slope of the fusion excitation functions at energies deep below the barrier. Mişicu and Esbensen [27, 28] constructed an ion-ion potential by double-folding method and added a repulsive core arising from nuclear incompressibility. Contrary to this *sudden* approach, Ichikawa et al. [29–31] proposed a smooth transition from sudden to *adiabatic* potential, as the densities of the participating nuclei begin to overlap, by imposing a damping factor on the coupling strength. Dasgupta *et al.* [32] suggested that the CC formalism may itself be inadequate at very low energies and a gradual onset of quantum decoherence need to be considered. A concise review of all the theoretical investigations on deep sub-barrier fusion hindrance can be found in Ref. [3]. Ichikawa and Matsuyanagi [33] has also argued that damping of quantum vibration in the reaction partners near the touching point is a universal mechanism which is causing hindrance to fusion deep below the barrier. Pauli exclusion principle has recently been included in the computation of the bare potential in a new microscopic approach called the density-constrained frozen Hartree-Fock method [34]. Pauli repulsion has been shown to reduce the tunneling probability, thus, offering partial explanation of observed hindrance to fusion.

Two different experimental techniques have been adopted to measure σ_{fus} at sub- μb levels. In the online technique, fusion products, *i.e.* the evaporation residues (ERs), are separated by an electromagnetic recoil separator and detected at a background-free site, usually the focal plane of the separator [19]. This technique, though direct and elegant, demands higher recoil energies of the ERs for their efficient detection. Consequently, fusion reactions between relatively lighter projectiles on heavier targets, in which ERs do not possess sufficient recoil energy, are difficult to study experimentally. The difficulty may be overcome in the off-beam characteristic γ -ray counting technique [35]. Measurements of σ_{fus} deep below the barrier have, so far, been reported for only a handful of asymmetric reactions primarily because of challenging experimental conditions.

Results from asymmetric reactions seem to suggest that fusion hindrance becomes increasingly significant

with increasing mass and charge of the projectiles. The reactions ${}^6,7\text{Li}+{}^{198}\text{Pt}$ [36, 37] showed no signs of fusion hindrance. Weak signature of fusion hindrance has recently been reported for the reaction ${}^{11}\text{B}+{}^{197}\text{Au}$ [38]. The reaction ${}^{12}\text{C}+{}^{198}\text{Pt}$ [37] exhibited clear sign of fusion hindrance. Significant hindrance to fusion had been reported in case of ${}^{16}\text{O}+{}^{204,208}\text{Pb}$ [32]. In all of these reactions measurement has been extended close to or below the threshold energy (see Table I), given by Eq. 3. One would, thus, expect to observe fusion hindrance in reactions between projectiles heavier than ${}^{16}\text{O}$ and heavy targets, below the threshold energy.

To investigate further the role of projectile mass and charge in fusion hindrance in asymmetric reactions, we extended the measurement of ER cross sections (σ_{ER}) for the system ${}^{19}\text{F}+{}^{181}\text{Ta}$ below the threshold energy. Measurements of σ_{ER} and σ_{fiss} for this reaction had been reported earlier [39–42]. σ_{fus} , which is a sum of σ_{ER} and σ_{fiss} was reported by Nasirov *et al.* [43] in the range of $E_{\text{lab}} = 80.0 - 120.0$ MeV. At $E_{\text{lab}} = 80$ MeV, σ_{fiss} is a negligible fraction of σ_{fus} . Hence, the σ_{ER} , reported in this work, can be taken as σ_{fus} for $E_{\text{lab}} < 80$ MeV.

The experiment was carried out in two runs at the 15UD Pelletron accelerator facility of IUAC, New Delhi. A pulsed ${}^{19}\text{F}$ beam, with pulse separation of 4 μs , was bombarded onto a 170 $\mu\text{g}/\text{cm}^2$ thick ${}^{181}\text{Ta}$ target on a 20 $\mu\text{g}/\text{cm}^2$ ${}^{\text{nat}}\text{C}$ backing. Measurements were performed at beam energies (E_{lab}) in the range of 73.7–123.8 MeV using the Heavy Ion Reaction Analyzer (HIRA) [44]. ERs formed in complete fusion of the reaction partners were separated from orders-of-magnitude larger background events by the HIRA. Two monitor detectors were placed at laboratory angle (θ_{lab}) 15.5° with respect to beam direction, in the horizontal plane, inside the target chamber for absolute normalization of σ_{ER} . A thin (30 $\mu\text{g}/\text{cm}^2$) ${}^{\text{nat}}\text{C}$ foil was placed 10 cm downstream from the target to reset ER charge states to equilibrium distribution. A multi-wire proportional counter (MWPC), having an active area of 15.0×5.0 cm^2 , was used to detect ERs at the focal plane of the HIRA. A very thin (0.5 μm) mylar foil was used as the entrance window of the MWPC, filled with isobutane at 3 mbar pressure, to minimize loss of energy for ERs. The HIRA was operated at 0° with 10 msr acceptance. Time interval between the arrival of a particle at the focal plane and the beam pulse was recorded as a measure of ER time of flight (TOF). Yield of ERs were extracted from the coincidence spectrum between energy loss (ΔE), obtained from the cathode of MWPC, and TOF.

The most challenging aspect of measuring σ_{fus} in this experiment was to identify the ERs unambiguously. It is clearly observed from Fig. 1 that separating the ERs from the scattered projectile-like particles becomes increasingly challenging with decreasing E_{lab} . Near the barrier ($E_{\text{lab}} = 85.7$ MeV), the ERs are clearly identified (Fig. 1.(a)). At $E_{\text{lab}} = 73.7$ MeV, ERs started merging with the background (Fig. 1.(e)), thus setting the lower energy limit in the present measurement. The other ma-

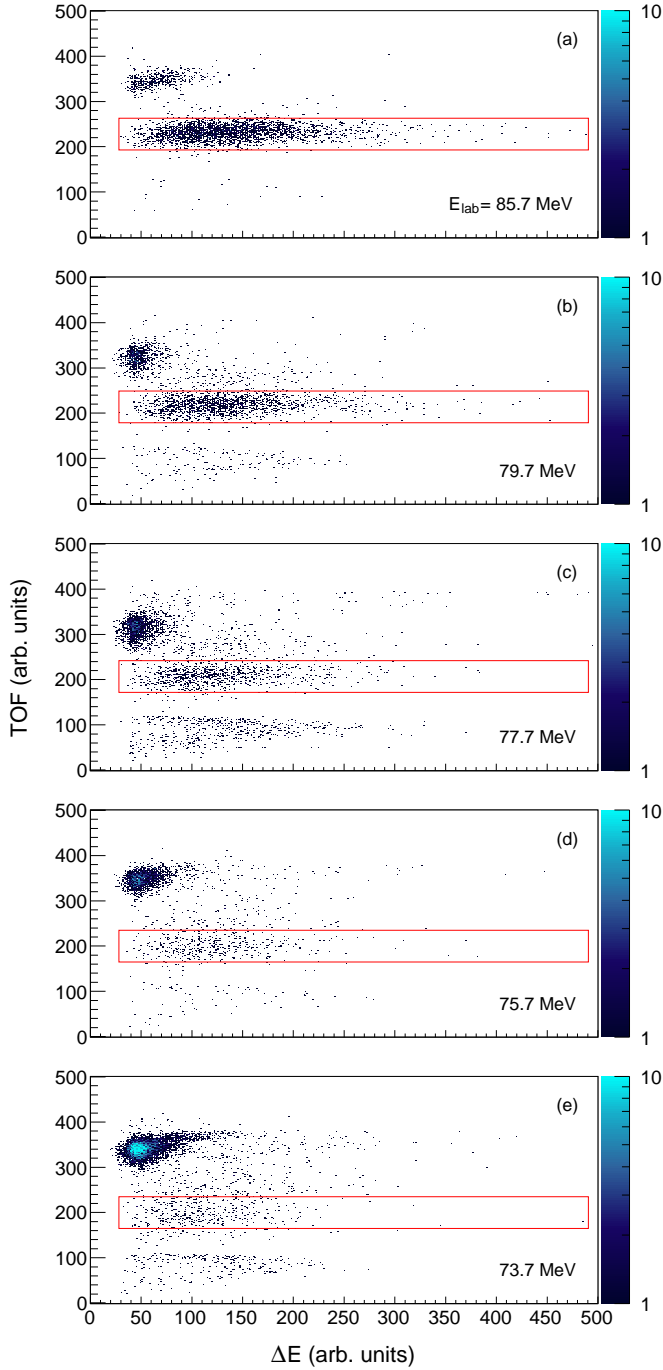


FIG. 1. (Color online) Scatter plots between ΔE and TOF of the events recorded at the focal plane of the HIRA for $^{19}\text{F} + ^{181}\text{Ta}$, from (a) $E_{\text{lab}} = 85.7$ MeV ($\frac{E_{\text{c.m.}}}{V_B} \simeq 1.01$) to (e) $E_{\text{lab}} = 73.7$ MeV ($\frac{E_{\text{c.m.}}}{V_B} \simeq 0.86$). V_B is the Coulomb barrier in c.m. frame of reference. ERs are enclosed within a rectangular gate in each panel. See text for details.

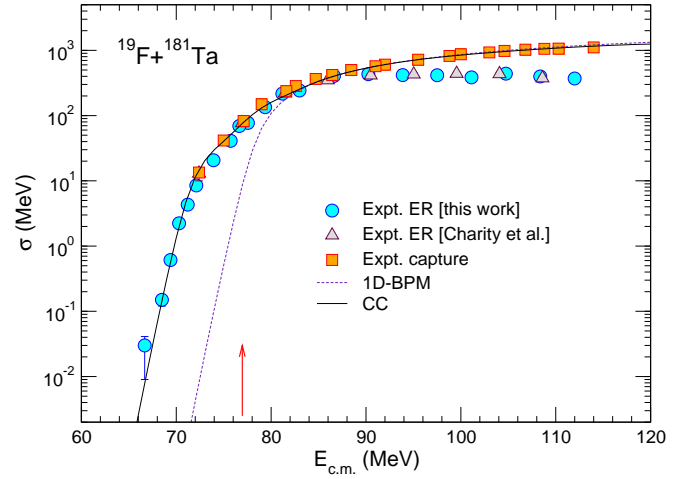


FIG. 2. (Color online) Measured σ_{ER} and σ_{fus} , as a function of $E_{\text{c.m.}}$, for the system $^{19}\text{F} + ^{181}\text{Ta}$. Data points shown with solid triangles had been reported by Charity *et al.* [41] whereas experimental σ_{fus} were obtained from Ref. [43]. Results from CC model calculation are also shown. The vertical arrow indicates position of the Coulomb barrier.

major challenge was to estimate the transmission efficiency of the HIRA (ϵ_{HIRA}) accurately, which is crucial for extraction of absolute σ_{ER} from data. ϵ_{HIRA} was calculated using the semi-microscopic Monte Carlo code TERS [45]. Details of the data analysis method can be found in Refs. [46, 47].

The previously measured σ_{fus} and σ_{ER} , along with data from the present investigation are presented in Fig. 2. One may note that data from this work match with data from the earlier measurement within the experimental uncertainties in the overlapping energy region. The experimental fusion excitation function has also been compared with the predictions of the coupled-channels code CCFULL [48] in Fig. 2. In the calculation, Woods-Saxon potential parameters, *viz.* depth (V_0), radius (r_0) and diffuseness (a), were chosen as 104.5 MeV, 1.12 fm and 0.70 fm, respectively, so as to reproduce the excitation function above the barrier. The output with no coupling configuration has been taken as the 1D-BPM cross sections. As both the target and the projectile are odd-even nuclei, the deformation parameters have been taken as the average of their neighboring even-even nuclei. It is observed from Fig. 2 that couplings have very insignificant effect at energies above the barrier and both 1D-BPM and CC predictions match with the experimental σ_{fus} . As energy decreases the 1D-BPM prediction starts to underestimate the experimental data. The coupling to the inelastic excitations of target and projectile describes the data quite satisfactorily up to the lowest energy reported in this work. Thus, no sign of fusion hindrance compared to CC prediction has been observed in the measured energy range.

To amplify any possible discrepancy between the experimental and theoretical fusion excitation functions in

the measured energy range, $L(E_{c.m.})$ has been plotted in Fig. 3(a). It is noted that the CC predictions explain the data quite satisfactorily throughout the measured energy range. No pronounced change of slope in the deep sub-barrier energy region is observed. The double-dot-dashed line represents the logarithmic derivative for a constant S -factor, $L_{CS}(E_{c.m.}) = \frac{\pi\eta}{E_{c.m.}}$ [18]. We observe that $L_{CS}(E_{c.m.})$ curve lies much above the data and the CC results. There is no cross-over between $L_{CS}(E_{c.m.})$ and $L(E_{c.m.})$, which is observed in systems exhibiting fusion hindrance [12, 37]. The intersection between these two curves is taken as the experimental threshold for fusion hindrance. Therefore, no threshold of fusion hindrance is observed for the reaction $^{19}\text{F}+^{181}\text{Ta}$ till $\simeq 12$ MeV below the barrier (equivalent $\simeq 0.86V_B$). $S(E_{c.m.})$ has been plotted in Fig. 3(b). Neither the maximum nor any saturation of the S -factor is observed within the measured energy range.

We next compare the observations for the system $^{19}\text{F}+^{181}\text{Ta}$ with results of other asymmetric systems mentioned earlier. The present reaction does not follow the systematic observations of increasingly stronger fusion hindrance with increasing mass and charge of the projectile. The contrast between the systems $^{16}\text{O}+^{204,208}\text{Pb}$ and $^{19}\text{F}+^{181}\text{Ta}$ is particularly striking. Hindrance to fusion starts showing up from $\simeq 5$ MeV below the barrier (equivalently $\simeq 0.94V_B$) for the ^{16}O -induced reaction, whereas no hindrance is observed even $\simeq 12$ MeV below the barrier (equivalently $\simeq 0.86V_B$) for the ^{19}F -induced reaction.

Recent theoretical investigations [33, 34] point to the generic nature of fusion hindrance deep below the barrier and acknowledge (a) gradual onset of decoherence, (b) transition from nucleus-nucleus sudden to one-nucleus adiabatic potential and (c) Pauli repulsion as the probable contributors in the phenomenon. In case of non-observation of fusion hindrance in a particular reaction one must, therefore, look into other factors which are specific to that reaction.

Break-up of the projectile and presence of light particle transfer channels are known to affect fusion between two nuclei. We note that the reactions showing no hindrance to fusion are induced by projectiles with low α -particle break-up threshold: 1.474 MeV, 2.468 MeV and 4.013 MeV for ^6Li , ^7Li and ^{19}F , respectively. On the other hand, reactions exhibiting fusion hindrance are induced by projectiles with much higher α -particle break-up threshold: 8.665 MeV, 7.366 MeV and 7.162 MeV for ^{11}B , ^{12}C and ^{16}O , respectively. n , $2n$, p , $2p$, ^2H , ^3H , ^3He and ^4He pick-up transfer Q -values for the asymmetric reactions are presented in Table I. One may also note in Table I that many of the particle transfer Q -values are positive for the reactions showing no fusion hindrance, *viz.* $^6,7\text{Li}+^{198}\text{Pt}$ and $^{19}\text{F}+^{181}\text{Pt}$. On the contrary, the reactions showing clearest signatures of fusion hindrance *i.e.* $^{12}\text{C}+^{198}\text{Pt}$ and $^{16}\text{O}+^{208}\text{Pb}$ have all but one negative particle transfer Q -values. We may, therefore, conclude that presence of break-up and particle transfer channels

are aiding in sub-barrier fusion. The effects of fusion hindrance, which is expected to be manifested in all reactions at energies below the threshold energy, appears to have been *compensated* in the presence of these direct reaction channels. A comprehensive theoretical investigation is needed to strengthen and quantify this conclusion.

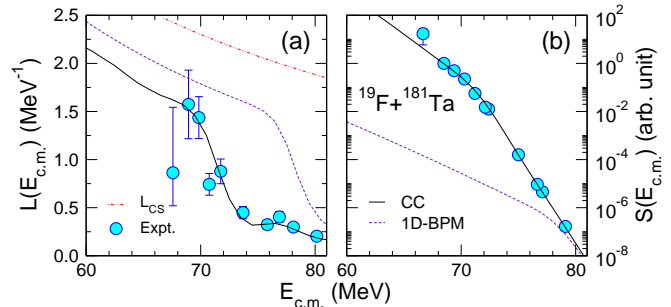


FIG. 3. (Color online) (a) The logarithmic derivative of the energy-weighted cross section and (b) the astrophysical S -factor, as a function of $E_{c.m.}$, for the system $^{19}\text{F} + ^{181}\text{Ta}$. Results from CC model calculation are also shown. The double-dot-dashed line in panel (a) represents the logarithmic derivative for a constant S -factor, $L_{CS}(E_{c.m.})$.

In summary, we have measured σ_{ER} for the reaction $^{19}\text{F}+^{181}\text{Ta}$ down to $\simeq 14\%$ below the barrier. As σ_{fiss} had earlier been shown to be insignificant below the barrier, σ_{ER} measured in this work has been considered as σ_{fus} at $E_{lab} < 80$ MeV. CC calculation with standard Woods-Saxon potential has reproduced σ_{fus} quite satisfactorily. Thus, fusion hindrance has not been observed in this reaction, though measurement has been extended below the threshold energy. We have compared our observation with results from other asymmetric reactions. It has been found that reactions induced by projectiles with low α -particle break-up threshold and having many light particles transfer channels with positive Q -values did not show fusion hindrance even below the threshold energy. On the other hand, reactions induced by strongly bound projectiles and having most of the light particles transfer channels with negative Q -values exhibited fusion hindrance. This is in contradiction with the recent observation of increasingly stronger fusion hindrance in asymmetric systems with increasing mass and charge of the projectile. Extending the measurement deeper below the barrier for $^{19}\text{F}+^{181}\text{Ta}$ and measuring σ_{fus} for more asymmetric systems will strengthen our conclusion. CC calculation including the effects of projectile break-up and particle transfer to reproduce fusion excitation functions deep below the barrier would complement the challenging experimental efforts.

The authors thank the Pelletron staff of IUAC for providing beams of excellent quality throughout the experiment, Mr. Abhilash S. R. for assistance in fabricating the target and Mr. T. Varughese for support during the experiment. The authors thank Mr. Rohan Biswas for useful discussions.

TABLE I. Details of the asymmetric systems considered in this work. E_{\min} is the lowest energy in the c.m. frame of reference at which measurement has been reported. Q_{CN} is the Q -value for compound nucleus formation. Q_x is the pick-up transfer Q -values, where x stand for n , $2n$, p , $2p$, ${}^2\text{H}$, ${}^3\text{H}$, ${}^3\text{He}$ and ${}^4\text{He}$.

System	$Z_p Z_t$	ζ	V_B (MeV)	E_s (MeV)	E_{\min} (MeV)	Q_{CN} (MeV)	Q_n (MeV)	Q_{2n} (MeV)	Q_p (MeV)	Q_{2p} (MeV)	$Q_{{}^2\text{H}}$ (MeV)	$Q_{{}^3\text{H}}$ (MeV)	$Q_{{}^3\text{He}}$ (MeV)	$Q_{{}^4\text{He}}$ (MeV)
${}^{19}\text{F}+{}^{181}\text{Ta}$	657	2724	77.9	69.4	66.7	-23.67	-0.98	0.48	6.90	1.32	6.27	10.53	5.59	11.99
${}^{16}\text{O}+{}^{208}\text{Pb}$ [32]	656	2529	77.0	66.1	68.7	-46.48	-3.22	-1.92	-7.40	-10.86	-5.11	-1.18	-5.95	5.25
${}^{16}\text{O}+{}^{204}\text{Pb}$ [32]	656	2527	77.3	66.0	68.7	-44.52	-4.25	-3.12	-6.04	-7.82	-4.74	-1.18	-3.94	6.70
${}^{12}\text{C}+{}^{198}\text{Pt}$ [37]	468	1574	56.0	48.2	47.0	-13.95	-2.61	-0.28	-6.99	-9.63	-3.33	1.69	-3.25	7.27
${}^{11}\text{B}+{}^{197}\text{Au}$ [38]	395	1275	47.4	41.9	37.9	5.00	-4.70	-6.47	10.17	3.87	7.20	9.27	7.20	11.96
${}^7\text{Li}+{}^{198}\text{Pt}$ [37]	234	608	28.5	25.6	19.3	8.82	-5.52	-7.31	8.33	0.86	3.09	4.09	2.46	8.77
${}^6\text{Li}+{}^{198}\text{Pt}$ [36]	234	565	28.9	24.3	19.6	8.53	-0.30	-4.12	-3.32	-10.46	8.68	4.53	1.28	4.57

- [1] M. Dasgupta, D. J. Hinde, N. Rowley, and A. M. Stefanini, *Ann. Rev. Part. Sci.* **48**, 401 (1998).
- [2] K. Hagino and N. Takigawa, *Prog. Theo. Phys.* **128**, 1061 (2012).
- [3] B. B. Back, H. Esbensen, C. L. Jiang, and K. E. Rehm, *Rev. Mod. Phys.* **86**, 317 (2014).
- [4] L. F. Canto, P. R. S. Gomes, R. Donangelo, J. Lubian, and M. S. Hussein, *Phys. Rep.* **596**, 1 (2015).
- [5] C. L. Jiang, H. Esbensen, K. E. Rehm, B. B. Back, R. V. F. Janssens, J. A. Caggiano, P. Collon, J. Greene, A. M. Heinz, D. J. Henderson, I. Nishinaka, T. O. Pennington, and D. Seweryniak, *Phys. Rev. Lett.* **89**, 052701 (2002).
- [6] C. L. Jiang, K. E. Rehm, B. B. Back, and R. V. F. Janssens, *Phys. Rev. C* **75**, 015803 (2007).
- [7] C. L. Jiang, K. E. Rehm, B. B. Back, and R. V. F. Janssens, *Phys. Rev. C* **79**, 044601 (2009).
- [8] C. L. Jiang, B. B. Back, H. Esbensen, J. P. Greene, R. V. F. Janssens, D. J. Henderson, H. Y. Lee, C. J. Lister, M. Notani, R. C. Pardo, N. Patel, K. E. Rehm, D. Seweryniak, B. Shumard, X. Wang, S. Zhu, Ş. Mişicu, P. Collon, and X. D. Tang, *Phys. Rev. C* **78**, 017601 (2008).
- [9] A. M. Stefanini, G. Montagnoli, R. Silvestri, S. Beghini, L. Corradi, S. Courtin, E. Fioretto, B. Guiot, F. Haas, D. Lehbertz, N. Mărginean, P. Mason, F. Scarlassara, R. N. Sagaidak, and S. Szilner, *Phys. Rev. C* **78**, 044607 (2008).
- [10] A. M. Stefanini, G. Montagnoli, R. Silvestri, L. Corradi, S. Courtin, E. Fioretto, B. Guiot, F. Haas, D. Lehbertz, P. Mason, F. Scarlassara, and S. Szilner, *Phys. Lett. B* **679**, 95 (2009).
- [11] C. L. Jiang, K. E. Rehm, H. Esbensen, B. B. Back, R. V. F. Janssens, P. Collon, C. M. Deibel, B. DiGiovine, J. M. Figueira, J. P. Greene, D. J. Henderson, H. Y. Lee, M. Notani, S. T. Marley, R. C. Pardo, N. Patel, D. Seweryniak, X. D. Tang, C. Ugalde, and S. Zhu, *Phys. Rev. C* **81**, 024611 (2010).
- [12] C. L. Jiang, A. M. Stefanini, H. Esbensen, K. E. Rehm, L. Corradi, E. Fioretto, P. Mason, G. Montagnoli, F. Scarlassara, R. Silvestri, P. P. Singh, S. Szilner, X. D. Tang, and C. A. Ur, *Phys. Rev. C* **82**, 041601(R) (2010).
- [13] G. Montagnoli, A. M. Stefanini, L. Corradi, S. Courtin, E. Fioretto, F. Haas, D. Lehbertz, F. Scarlassara, R. Silvestri, and S. Szilner, *Phys. Rev. C* **82**, 064609 (2010).
- [14] G. Montagnoli, F. Scarlassara, P. Mason, A. M. Stefanini, R. Silvestri, L. Corradi, E. Fioretto, B. Guiot, S. Courtin, F. Haas, D. Lehbertz, and S. Szilner *Nucl. Phys. A* **834**, 159 (2010).
- [15] G. Montagnoli, A. M. Stefanini, C. L. Jiang, H. Esbensen, L. Corradi, S. Courtin, E. Fioretto, A. Goasduff, F. Haas, A. F. Kifle, C. Michelagnoli, D. Montanari, T. Mijatović, K. E. Rehm, R. Silvestri, Pushpendra P. Singh, F. Scarlassara, S. Szilner, X. D. Tang, and C. A. Ur, *Phys. Rev. C* **85**, 024607 (2012).
- [16] G. Montagnoli, A. M. Stefanini, H. Esbensen, C. L. Jiang, L. Corradi, S. Courtin, E. Fioretto, A. Goasduff, J. Grebosz, F. Haas, M. Mazzocco, C. Michelagnoli, T. Mijatović, D. Montanari, C. Parascandolo, K. E. Rehm, F. Scarlassara, S. Szilner, X. D. Tang, and C. A. Ur, *Phys. Rev. C* **87**, 014611 (2013).
- [17] C. L. Jiang, A. M. Stefanini, H. Esbensen, K. E. Rehm, S. Almaraz-Calderon, B. B. Back, L. Corradi, E. Fioretto, G. Montagnoli, F. Scarlassara, D. Montanari, S. Courtin, D. Bourgin, F. Haas, A. Goasduff, S. Szilner, and T. Mijatović, *Phys. Rev. Lett.* **113**, 022701 (2014).
- [18] C. L. Jiang, K. E. Rehm, R. V. F. Janssens, H. Esbensen, I. Ahmad, B. B. Back, P. Collon, C. N. Davids, J. P. Greene, D. J. Henderson, G. Mukherjee, R. C. Pardo, M. Paul, T. O. Pennington, D. Seweryniak, S. Sinha, and Z. Zhou, *Phys. Rev. Lett.* **93**, 012701 (2004).
- [19] C. L. Jiang, K. E. Rehm, H. Esbensen, R. V. F. Janssens, B. B. Back, C. N. Davids, J. P. Greene, D. J. Henderson, C. J. Lister, R. C. Pardo, T. Pennington, D. Peterson, D. Seweryniak, B. Shumard, S. Sinha, X. D. Tang, I. Tanihata, S. Zhu, P. Collon, S. Kurtz, and M. Paul, *Phys. Rev. C* **71**, 044613 (2005).
- [20] C. L. Jiang, B. B. Back, H. Esbensen, R. V. F. Janssens, Ş. Mişicu, K. E. Rehm, P. Collon, C. N. Davids, J. Greene, D. J. Henderson, L. Jisonna, S. Kurtz, C. J. Lister, M. Notani, M. Paul, R. Pardo, D. Peterson, D. Seweryniak, B. Shumard, X. D. Tang, I. Tanihata, X. Wang, and S. Zhu, *Phys. Lett. B* **640**, 18 (2006).
- [21] A. M. Stefanini, G. Montagnoli, L. Corradi, S. Courtin, E. Fioretto, A. Goasduff, F. Haas, P. Mason, R. Silvestri, Pushpendra P. Singh, F. Scarlassara, and S. Szilner, *Phys. Rev. C* **82**, 014614 (2010).
- [22] A. M. Stefanini, G. Montagnoli, L. Corradi, S. Courtin, D. Bourgin, E. Fioretto, A. Goasduff, J. Grebosz, F. Haas, M. Mazzocco, T. Mijatović, D. Montanari, M. Pagliaroli, C. Parascandolo, F. Scarlassara, E. Strano, S. Szilner, N. Toniolo, and D. Torresi, *Phys. Rev. C* **92**,

- 064607 (2015).
- [23] A. M. Stefanini, F. Scarlassara, S. Beghini, G. Montagnoli, R. Silvestri, M. Trotta, B. R. Behera, L. Corradi, E. Fioretto, A. Gadea, Y. W. Wu, S. Szilner, H. Q. Zhang, Z. H. Liu, M. Ruan, F. Yang, and N. Rowley, *Phys. Rev. C* **73**, 034606 (2006).
- [24] A. M. Stefanini, B. R. Behera, S. Beghini, L. Corradi, E. Fioretto, A. Gadea, G. Montagnoli, N. Rowley, F. Scarlassara, S. Szilner, and M. Trotta, *Phys. Rev. C* **76**, 014610 (2007).
- [25] A. M. Stefanini, G. Montagnoli, H. Esbensen, P. Čolović, L. Corradi, E. Fioretto, F. Galtarossa, A. Goasduff, J. Grebosz, F. Haas, M. Mazzocco, N. Soić, E. Strano, and S. Szilner, *Phys. Rev. C* **96**, 014603 (2017).
- [26] C. L. Jiang, H. Esbensen, B. B. Back, R. V. F. Janssens, and K. E. Rehm, *Phys. Rev. C* **69**, 014604 (2004).
- [27] Š. Mišicu and H. Esbensen, *Phys. Rev. Lett.* **96**, 112701 (2006).
- [28] Š. Mišicu and H. Esbensen, *Phys. Rev. C* **75**, 034606 (2007).
- [29] Takatoshi Ichikawa, Kouichi Hagino, and Akira Iwamoto, *Phys. Rev. C* **75**, 057603 (2007).
- [30] Takatoshi Ichikawa, Kouichi Hagino, and Akira Iwamoto, *Phys. Rev. Lett.* **103**, 202701 (2009).
- [31] Takatoshi Ichikawa, *Phys. Rev. C* **92**, 064604 (2015).
- [32] M. Dasgupta, D. J. Hinde, A. Diaz-Torres, B. Bouriquet, Catherine I. Low, G. J. Milburn, and J. O. Newton, *Phys. Rev. Lett.* **99**, 192701 (2007).
- [33] Takatoshi Ichikawa and Kenichi Matsuyanagi, *Phys. Rev. C* **2**, 021602(R) (2015).
- [34] C. Simenel, A. S. Umar, K. Godbey, M. Dasgupta, and D. J. Hinde, *Phys. Rev. C* **95**, 031601(R) (2017).
- [35] A. Lemasson, A. Shrivastava, A. Navin, M. Rejmund, V. Nanal, S. Bhattacharyya, A. Chatterjee, S. Kailas, K. Mahata, V. V. Parkar, R. G. Pillay, K. Ramachandran, and P. C. Rout, *Nucl. Instrum. Methods A* **598**, 445 (2009).
- [36] A. Shrivastava, A. Navin, A. Lemasson, K. Ramachandran, V. Nanal, M. Rejmund, K. Hagino, T. Ichikawa, S. Bhattacharyya, A. Chatterjee, S. Kailas, K. Mahata, V. V. Parkar, R. G. Pillay, and P. C. Rout, *Phys. Rev. Lett.* **103**, 232702 (2009).
- [37] A. Shrivastava, K. Mahata, S. K. Pandit, V. Nanal, T. Ichikawa, K. Hagino, A. Navin, C. S. Palshetkar, V. V. Parkar, K. Ramachandran, P. C. Rout, Abhinav Kumar, A. Chatterjee, and S. Kailas, *Phys. Lett. B* **755**, 332 (2016).
- [38] A. Shrivastava, K. Mahata, V. Nanal, S. K. Pandit, V. V. Parkar, P. C. Rout, N. Dokania, K. Ramachandran, A. Kumar, A. Chatterjee, and S. Kailas, *Phys. Rev. C* **96**, 034620 (2017).
- [39] J. R. Leigh, D. J. Hinde, J. O. Newton, W. Galster, and S. H. Sie, *Phys. Rev. Lett.* **48**, 527 (1982).
- [40] D. J. Hinde, J. R. Leigh, J. O. Newton, W. Galster, and S. Sie, *Nucl. Phys A* **385**, 109 (1982).
- [41] R. J. Charity, J. R. Leigh, J. J. M. Bokhorst, A. Chatterjee, G. S. Foote, D. J. Hinde, J. O. Newton, S. Ogaza, and D. Ward, *Nucl. Phys A* **457**, 441 (1986).
- [42] A. L. Caraley, B. P. Henry, J. P. Lestone, and R. Vandenbosch, *Phys. Rev. C* **62**, 054612 (2000).
- [43] A. K. Nasirov, G. Mandaglio, M. Manganaro, A. I. Muminov, G. Fazio, and G. Giardina, *Phys. Lett. B* **686**, 72 (2010).
- [44] A. K. Sinha, N. Madhavan, J. J. Das, P. Sugathan, D. O. Kataria, A. P. Patro, and G. K. Mehta, *Nucl. Instrum. Methods A* **339**, 543 (1994).
- [45] S. Nath, *Comput. Phys. Commun.* **179**, 492 (2008); **180**, 2392 (2009).
- [46] S. Nath, P. V. Madhusudhana Rao, S. Pal, J. Gehlot, E. Prasad, G. Mohanto, S. Kalkal, J. Sadhukhan, P. D. Shidling, K. S. Golda, A. Jhingan, N. Madhavan, S. Muralithar, and A. K. Sinha, *Phys. Rev. C* **81**, 064601 (2010).
- [47] Tapan Rajbongshi, K. Kalita, S. Nath, J. Gehlot, Tathagata Banerjee, Ish Mukul, R. Dubey, N. Madhavan, C. J. Lin, A. Shamlath, P. V. Laveen, M. Shareef, Neeraj Kumar, P. Jisha, and P. Sharma, *Phys. Rev. C* **93**, 054622 (2016).
- [48] K. Hagino, N. Rowley, and A. T. Kruppa, *Comput. Phys. Commun.* **123**, 143 (1999).